OPEN ACCESS Freely available online

PLoS one

C/EBPβ Promotes Transition from Proliferation to Hypertrophic Differentiation of Chondrocytes through Transactivation of $p57^{Kip2}$

Makoto Hirata[1¶], Fumitaka Kugimiya[1¶], Atsushi Fukai[1], Shinsuke Ohba[2], Naohiro Kawamura[1], Toru Ogasawara[1], Yosuke Kawasaki[1], Taku Saito[1], Fumiko Yano[2], Toshiyuki Ikeda[1], Kozo Nakamura[1], Ung-il Chung[2], Hiroshi Kawaguchi[1]*

1 Departments of Sensory & Motor System Medicine, Faculty of Medicine, University of Tokyo, Bunkyo-ku, Tokyo, Japan, 2 Center for Disease Biology and Integrative Medicine, Faculty of Medicine, University of Tokyo, Bunkyo-ku, Tokyo, Japan

Abstract

Background: Although transition from proliferation to hypertrophic differentiation of chondrocytes is a crucial step for endochondral ossification in physiological skeletal growth and pathological disorders like osteoarthritis, the underlying mechanism remains an enigma. This study investigated the role of the transcription factor CCAAT/enhancer-binding protein β (C/EBPβ) in chondrocytes during endochondral ossification.

Methodology/Principal Findings: Mouse embryos with homozygous deficiency in C/EBPβ (C/EBPβ−/−) exhibited dwarfism with elongated proliferative zone and delayed chondrocyte hypertrophy in the growth plate cartilage. In the cultures of primary C/EBPβ−/− chondrocytes, cell proliferation was enhanced while hypertrophic differentiation was suppressed. Contrarily, retroviral overexpression of C/EBPβ in chondrocytes suppressed the proliferation and enhanced the hypertrophy, suggesting the cell cycle arrest by C/EBPβ. In fact, a DNA cell cycle histogram revealed that the C/EBPβ overexpression caused accumulation of cells in the G0/G1 fraction. Among cell cycle factors, microarray and real-time RT-PCR analyses have identified the cyclin-dependent kinase inhibitor $p57^{Kip2}$ as the transcriptional target of C/EBPβ. $p57^{Kip2}$ was co-localized with C/EBPβ in late proliferative and pre-hypertrophic chondrocytes of the mouse growth plate, which was decreased by the C/EBPβ deficiency. Luciferase-reporter and electrophoretic mobility shift assays identified the core responsive element of C/EBPβ in the $p57^{Kip2}$ promoter between −150 and −130 bp region containing a putative C/EBP motif. The knockdown of $p57^{Kip2}$ by the siRNA inhibited the C/EBPβ-induced chondrocyte hypertrophy. Finally, when we created the experimental osteoarthritis model by inducing instability in the knee joints of adult mice of wild-type and C/EBPβ+/− littermates, the C/EBPβ insufficiency caused resistance to joint cartilage destruction.

Conclusions/Significance: C/EBPβ transactivates $p57^{Kip2}$ to promote transition from proliferation to hypertrophic differentiation of chondrocytes during endochondral ossification, suggesting that the C/EBPβ-$p57^{Kip2}$ signal would be a therapeutic target of skeletal disorders like growth retardation and osteoarthritis.

Citation: Hirata M, Kugimiya F, Fukai A, Ohba S, Kawamura N, et al. (2009) C/EBPβ Promotes Transition from Proliferation to Hypertrophic Differentiation of Chondrocytes through Transactivation of $p57^{Kip2}$. PLoS ONE 4(2): e4543. doi:10.1371/journal.pone.0004543

Editor: Thomas Zwaka, Baylor College of Medicine, United States of America

Received September 29, 2008; **Accepted** January 6, 2009; **Published** February 20, 2009

Funding: This study was supported by a Grant-in-aid for Scientific Research from the Japanese Ministry of Education, Culture, Sports, Science, and Technology (#19109007). The sponsor had no role in study design, data collection, data analysis, data interpretation, or writing of the manuscript.

Competing Interests: The authors have declared that no competing interests exist.

* E-mail: kawaguchi-ort@h.u-tokyo.ac.jp

¶ These authors contributed equally to this work.

Introduction

Most skeletal growth is achieved by endochondral ossification. During the process, chondrocytes undergo proliferation, hypertrophic differentiation, and apoptosis [1], each of which is regulated by distinct signals. Among them, chondrocyte hypertrophy is a rate-limiting step for the skeletal growth, being responsible for 40–60% of the endochondral ossification [2,3]. The initiation is precisely linked with the cessation of proliferation; however, the molecular mechanism underlying the harmonious transition from the proliferation to hypertrophic differentiation of chondrocytes remains an enigma.

CCAAT/enhancer-binding protein β (C/EBPβ), also known as nuclear factor-interleukin-6 (NF-IL6), is a member of the C/EBP family of six transcription factors characterized by a carboxyl-terminal leucine zipper dimerization domain and an adjacent highly conserved basic DNA binding domain [4–6]. Contrary to C/EBPα that is purely antiproliferative as a tumor suppressor in several cell types, C/EBPβ regulates expression of various genes involved in cell differentiation, proliferation, survival, immune function and female reproduction, as well as tumor invasiveness and progression, through a variety of mechanisms [6]. Over the past several years, C/EBPβ has been shown to control differentiation of hematopoietic and adipogenic cells [7,8]. The

present study initially investigated skeletal phenotype of C/EBPβ-deficient (C/EBPβ−/−) mice which have been reported to display mainly hematopoietic and adipogenic defects [9–11]. The mice showed dwarfism with an elongated proliferative zone and delayed chondrocyte hypertrophy in the limb cartilage, implicating the cell cycle control by C/EBPβ in chondrocytes.

Cell cycle factors appear to play an important role in the control of chondrocyte proliferation and differentiation [12,13]. During the cell cycle activation, complexes of cyclin and cyclin-dependent kinase (CDK) promote G1/S-phase transition from G0/G1 by phosphorylating Rb-related pocket proteins, which activate genes required for the S-phase entry. The cyclin-CDK complexes are inhibited by two major families of CDK inhibitors [14]. The p16 INK4 family specifically binds and inactivates monomeric CDK4 or CDK6, whereas the Cip/Kip family, which includes $p21^{Cip1}$, $p27^{Kip1}$, and $p57^{Kip2}$ (p57), inhibits all G1/S-phase cyclin-CDK complexes. Since the control of these cell cycle factors driving S-phase onset greatly influences the commitment to cell differentiation, the present study performed a screen of potential transcriptional targets of C/EBPβ using a microarray analysis, and identified p57 as the most probable target during hypertrophic differentiation of chondrocytes. We further investigated the molecular mechanism underlying the regulation of skeletal growth and endochondral ossification through the C/EBPβ-p57 signal in chondrocytes.

Results

C/EBPβ−/− mice exhibit impaired skeletal growth and endochondral ossification

To analyze the physiological role of C/EBPβ in skeletal growth and endochondral ossification, we investigated the skeletal phenotypes of heterozygous and homozygous C/EBPβ-deficient (C/EBPβ+/− and C/EBPβ−/−) mice. Although the C/EBPβ+/− skeleton was normal, C/EBPβ−/− mice exhibited dwarfism as compared to the wild-type littermates from embryonic stages (Figure 1A). After birth, however, the skeletal size of C/EBPβ−/− mice gradually caught up with that of the wild type littermates (Figure 1B), and they became similar after 1 week of age. At the embryos, the limbs and vertebrae which are known to be primarily formed through endochondral ossification were about 20–25% shorter in C/EBPβ−/− mice than the wild-type, although calvarial growth, especially the width, formed through endochondral ossification and intramembranous ossification did not show such a difference (Figure 1D). Skeletal double staining revealed that not only the total bone length, but also the ratio of mineralized area shown by the positive Alizarin red staining to the total length was decreased, confirming that endochondral ossification was impaired by the C/EBPβ deficiency (Figure 1C, E).

Hypertrophic differentiation of chondrocytes is delayed in the C/EBPβ−/− limb cartilage

To know the mechanism underlying the impaired skeletal growth in C/EBPβ−/− mice, we compared the tibial limb cartilage of the wild-type and C/EBPβ−/− littermates at E16.5 (Figure 2A). Among the resting, proliferative, hypertrophic zones, and bone area, the proliferative zone was elongated while the hypertrophic zone was normal in the C/EBPβ−/− limb (Figure 2B). The number of proliferating chondrocytes with BrdU uptake was actually increased in the C/EBPβ−/− cartilage (Figure 2C).

C/EBPβ was shown by immunohistochemistry to be localized predominantly in late proliferative and pre-hypertrophic chondrocytes of the wild-type cartilage, but not in the C/EBPβ−/− cartilage (Figure 2D, top). Further histological examination by BrdU labeling, in situ hybridization of type X collagen (COL10), immunohistochemistry of indian hedgehog (Ihh), and Alcian blue/von Kossa double stainings supported the elongation of the proliferative zone and delay of chondrocyte hypertrophy by the C/EBPβ deficiency (Figure 2D).

C/EBPβ inhibits proliferation and promotes hypertrophic differentiation in cultured primary chondrocytes

When primary chondrocytes derived from mouse ribs and mouse chondrogenic cell line ATDC5 were cultured in the differentiation medium, the C/EBPβ mRNA level was increased with the differentiation (Figure 3A), which was comparable to the in vivo expression pattern of the limb cartilage.

We then examined the effects of loss- and gain-of-functions of C/EBPβ on proliferation and hypertrophic differentiation of the primary rib chondrocytes. When chondrocytes from wild-type and C/EBPβ−/− littermates were compared, cell number determined by the XTT assay was enhanced in the C/EBPβ−/− chondrocytes at 3 d of culture (Figure 3B). The percentage of BrdU-positive cells was also increased in the C/EBPβ−/− culture at this time point (Figure 3C), indicating that the increased cell number was due to the enhanced proliferation, rather than the effect on cell survival, vitality, or apoptosis. Contrarily, hypertrophic differentiation determined by alkaline phosphatase (ALP) and Alizarin red stainings, and mRNA levels of COL10, matrix metalloproteinease-13 (MMP13) and vascular endothelial growth factor (VEGF), parameters of chondrocyte hypertrophy, were suppressed by the deficiency (Figure 3D).

In contrast, retroviral overexpression of C/EBPβ in the wild-type rib chondrocytes suppressed the proliferation and enhanced the hypertrophic differentiation parameters (Figure 3E, F, and G). Collectively, C/EBPβ was shown to be essential for cessation of proliferation and promotion of hypertrophic differentiation, suggesting arrest of the cell cycle and exit from it.

C/EBPβ regulates cell cycle and p57 as the transcriptional target

We therefore examined the regulation of cell cycle by C/EBPβ. A DNA cell cycle histogram in mouse mesenchymal C3H10T1/2 cells after the cycle synchronization revealed that the C/EBPβ overexpression enhanced accumulation of cells in the G0/G1 fraction (Figure 4A). To identify cell cycle factors lying downstream of the C/EBPβ signal, we performed a screen of transcriptional targets of C/EBPβ using a microarray analysis (Table S1). The C/EBPβ overexpression caused downregulation of cyclin B1, B2 and D1, and upregulation of the cyclin-dependent kinase inhibitors p16, p21 and p57, by 50% or more as compared to the empty vector overexpression. Since the above analyses were performed in non-chondrogenic C3H10T1/2 cells, we further examined the expressions of the candidate genes by real-time RT-PCR analysis in the cultures between wild-type and C/EBPβ−/− rib chondrocytes (Figure 4B). Cyclin B1, B2, and p21 were not significantly altered by the C/EBPβ deficiency, while p16 showed contradictory upregulation. Cyclin D1 and p57 were confirmed to be upregulated and downregulated, respectively, by the loss-of-function of C/EBPβ. However, when the expressions were further compared between primary chondrocytes with retroviral overexpression of C/EBPβ and the control GFP, the cyclin D1 was not downregulated, whereas p57 was upregulated by the C/EBPβ overexpression. These indicate that p57 was the only cell cycle factor whose expression was confirmed to be regulated positively and negatively by the gain- and loss-of-functions of C/EBPβ, respectively. Double immunofluorescence of p57 and BrdU in the

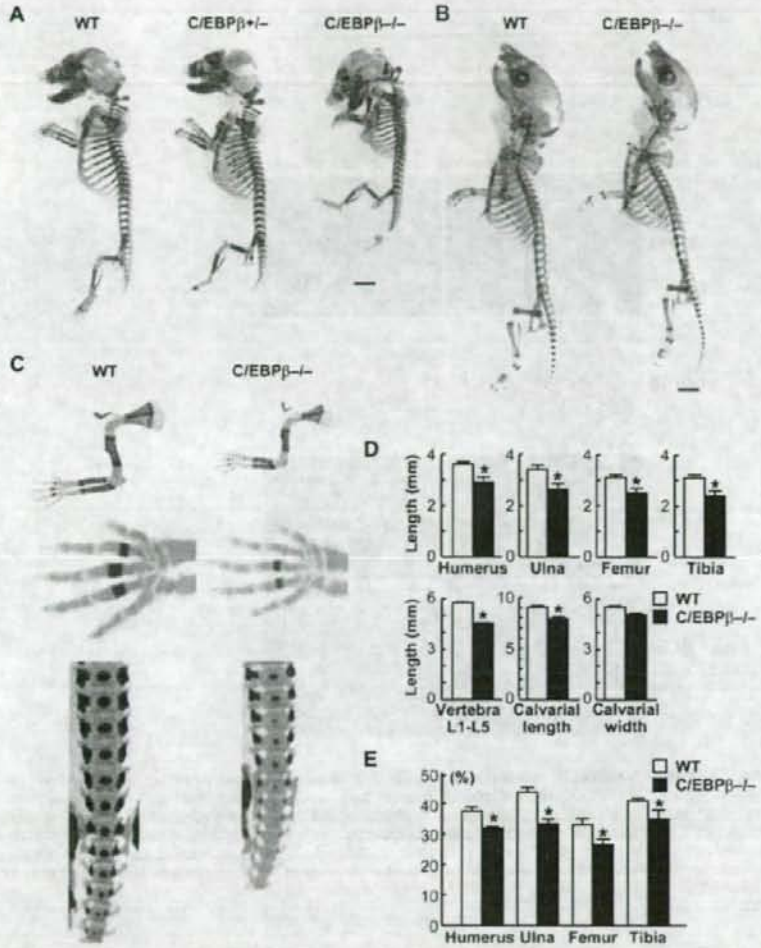

Figure 1. C/EBPβ−/− mice exhibit impaired skeletal growth and endochondral ossification. (A, B) Double stainings with Alizarin red and Alcian blue of the whole skeleton of the wild-type (WT), C/EBPβ+/−, and C/EBPβ−/− littermates at E16.5 (A) and at 3 d after birth (B). Scale bar, 2 mm. (C) Double stainings of the upper limbs, hands, and lumbar spines of the two genotypes. (D) Length of humerus, ulna, femur, tibia, vertebra (1st to 5th lumbar spines), and the calvarial length and width of the WT and C/EBPβ−/− littermates. (E) The percent ratio of Alizarin red-positive mineralized area to total length of the long bones of the two genotypes. Data are expressed as means (bars) ± SEM (error bars) of 4 bones per genotype. *$P<0.01$ vs. WT.

doi:10.1371/journal.pone.0004543.g001

wild-type cartilage revealed that p57 was localized predominantly in late proliferative and pre-hypertrophic chondrocytes which do not exhibit BrdU uptake (Figure 4C). The p57 expression was confirmed to be decreased in the C/EBPβ−/− cartilage.

C/EBPβ transactivates p57 through direct binding to a C/EBP motif

To know the mechanism underlying the induction of p57 expression by C/EBPβ, we analyzed the promoter activity of p57 using human hepatoma HuH-7 cells and ATDC5 cells transfected with a luciferase reporter gene construct containing the 5′-flanking sequences from −1,092 to +226 bp of the p57 promoter (Figure 5A). The transcriptional activity determined by the luciferase-reporter assay was enhanced by co-transfection with C/EBPβ in both cells, indicating the transcriptional induction of p57 by C/EBPβ. Deletion analysis by a series of 5′-deletion constructs identified the responsive element to C/EBPβ as being located between −150 and −130 bp region. The tandem-repeat constructs of this region were confirmed to respond to the C/EBPβ overexpression depending on the repeat number in both cells (Figure 5B). As this region contained a putative C/EBP-binding motif [15], the site-directed mutagenesis was carried out by creating two mutations in the motif. Both of the mutations caused partial but significant suppression of the promoter activity in both cells, indicating that the C/EBP motif is a responsive

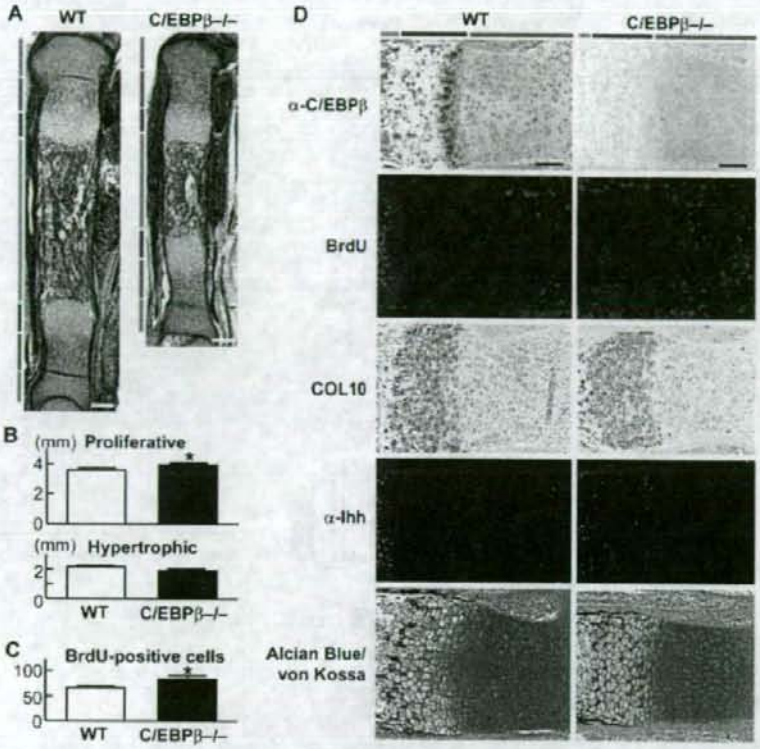

Figure 2. Hypertrophic differentiation of chondrocytes is delayed in the C/EBPβ−/− limb cartilage. (A) HE staining of whole tibias of wild-type (WT) and C/EBPβ−/− littermate embryos (E16.5). Orange, red, blue, and green bars indicate layers of resting zone, proliferative zone, hypertrophic zone, and bone area, respectively. Scale bars, 200 μm. (B) Length of proliferative and hypertrophic zones of the two genotypes. (C) Number of BrdU-positive cells in the proximal tibia of the two genotypes. Data are expressed as means (bars) ± SEM (error bars) of 5 mice per genotype. *$P<0.05$ vs. WT. (D) Immunostaining with an antibody to C/EBPβ (α-C/EBPβ), BrdU labeling, in situ hybridization of type X collagen (COL10), immunostaining with an antibody to Ihh (α-Ihh), and Alcian blue/von Kossa double stainings of the tibial cartilage in two genotypes. Color bars indicate layers as above. Scale bars, 100 μm.
doi:10.1371/journal.pone.0004543.g002

element (Figure 5C). EMSA revealed the specific binding of the nuclear extract from C/EBPβ-overexpressed ATDC5 cells with the oligonucleotide probe containing the identified responsive element above (Figure 5D). The mutagenesis in the C/EBP motif of the probe resulted in a failure to form the complex. Cold competition with excess amounts of an unlabeled wild-type probe, but not the mutated probe, suppressed the complex formation, confirming the specific binding to the C/EBPβ motif. Specificity of C/EBPβ binding was further verified by the antibody supershift. These lines of results demonstrate that C/EBPβ transactivates the p57 promoter, at least in part, through direct binding to a C/EBP motif between the −150 and −130 bp region.

The C/EBPβ-p57 signal induces chondrocyte hypertrophic differentiation

To know the functional interaction between C/EBPβ and p57 during chondrocyte hypertrophic differentiation, we established two small interfering RNA (siRNA) constructs of p57 for the gene silencing. We initially confirmed significant decreases of p57 protein and mRNA levels by stable transfection of the two siRNAs (Figure 5E). The C/EBPβ-induced hypertrophic differentiation of cultured rib chondrocytes determined by ALP staining and COL10 expression was suppressed by the p57 knockdown through the siRNA (Figure 5F), indicating the mediation of p57 in the C/EBPβ induction of hypertrophic differentiation. We confirmed that retroviral overexpression of p57 enhanced the hypertrophy markers in cultured ATDC5 cells (Figure 5G).

C/EBPβ is involved in cartilage destruction during osteoarthritis progression

In addition to the physiological role in skeletal growth in embryos, we finally examined the contribution of C/EBPβ in chondrocytes under pathological conditions. We and others have reported that endochondral ossification including chondrocyte hypertrophy is a crucial step for cartilage destruction during osteoarthritis progression [16 20]. We therefore created an experimental osteoarthritis model that induces instability to the knee joints in 8-week-old wild-type mice [17,21], and found that C/EBPβ was localized at the frontline of cartilage degradation in the central and peripheral areas of the joint cartilage during osteoarthritis progression (Figure 6A). To know the functional involvement of C/EBPβ under the pathological conditions, we

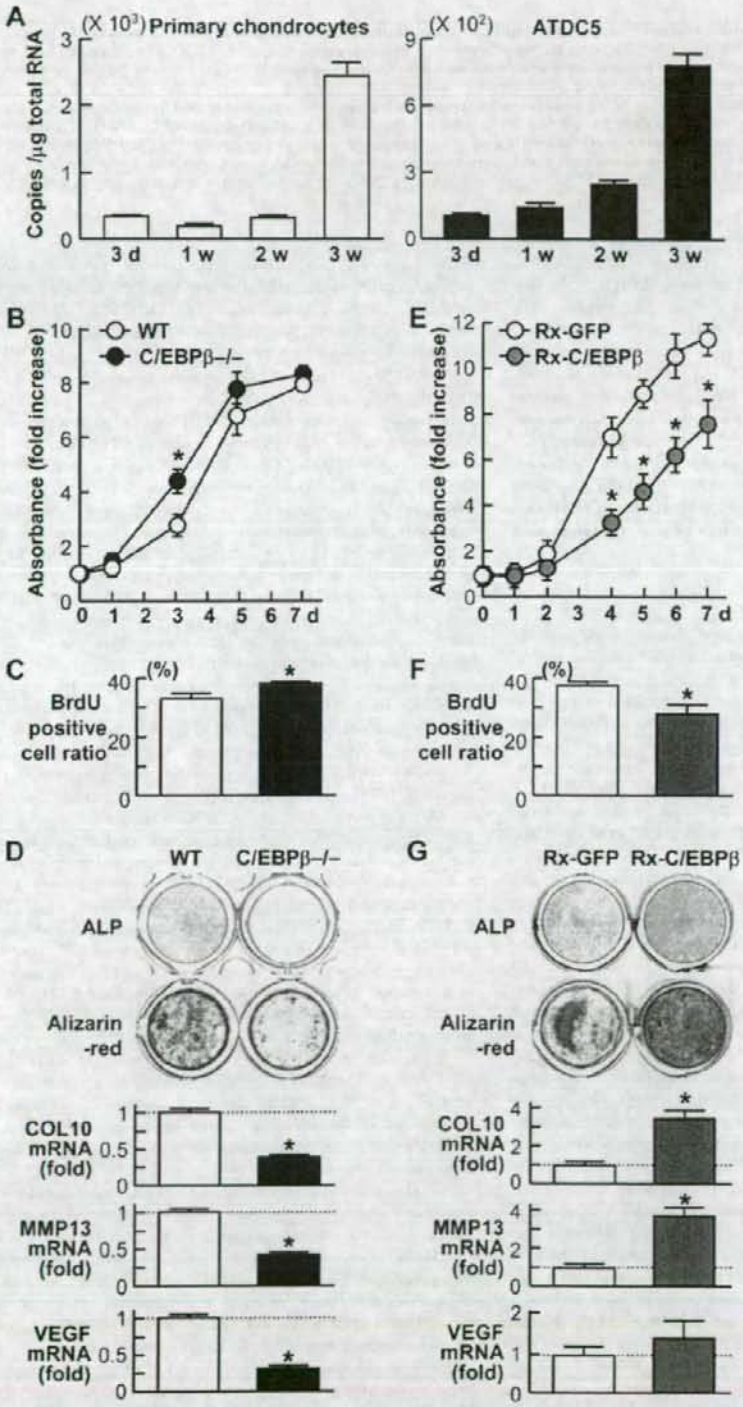
A
(X 10³) Primary chondrocytes
(X 10²) ATDC5
Copies /μg total RNA
3 d
1 w
2 w
3 w
B
WT
C/EBPβ–/–
Absorbance (fold increase)
E
Rx-GFP
Rx-C/EBPβ
C
BrdU positive cell ratio
(%)
F
D
WT
C/EBPβ–/–
ALP
Alizarin -red
COL10 mRNA (fold)
MMP13 mRNA (fold)
VEGF mRNA (fold)
G
Rx-GFP
Rx-C/EBPβ

Figure 3. C/EBPβ inhibits proliferation and promotes hypertrophic differentiation in cultured primary chondrocytes. (A) Time course of C/EBPβ mRNA level determined by real-time RT-PCR analysis during differentiation of primary chondrocytes and ATDC5 cells cultured for 3 weeks with insulin. (B) Growth curves by the XTT assay of primary chondrocytes derived from ribs of wild-type (WT) and C/EBPβ−/− littermates. (C) Ratio of BrdU-positive cells to total cells after 3 d culture of primary chondrocytes derived from WT and C/EBPβ−/− ribs. (D) ALP and Alizarin red stainings, and relative mRNA levels of COL10, MMP13, and VEGF of the primary chondrocytes from the two genotypes determined by real-time RT-PCR analysis at 2 weeks of culture after confluency. (E) Growth curves of primary WT rib chondrocytes with retroviral transfection of C/EBPβ (Rx-C/EBPβ) or the control GFP (Rx-GFP). (F) Ratio of BrdU-positive cells to total cells after 4 d culture of primary WT rib chondrocytes with Rx-C/EBPβ or Rx-GFP. (G) ALP and Alizarin red stainings, and relative mRNA levels of the chondrocyte hypertrophy markers of the rib chondrocytes with Rx-C/EBPβ or Rx-GFP at 2 weeks of culture after confluency. All data are expressed as means (symbols or bars) ± SEM (error bars) of 6 wells or dishes per group. *P<0.01 vs. WT or Rx-GFP.
doi:10.1371/journal.pone.0004543.g003

compared the cartilage destruction between C/EBPβ+/− and the wild-type littermates that showed similar phenotypes under physiological conditions (Figure 1A) [9]. C/EBPβ−/− mice were not used in this experiment since their skeleton was originally small, the joint shape was abnormal, and the activity was low, so that mechanical stress caused by the joint instability was not assumed to be comparable to that of wild-type mice. The cartilage destruction as well as COL10 expression was suppressed in C/EBPβ+/− mice, remaining a substantial undegraded matrix even 8 to 12 weeks after the surgery (Figure 6B). Quantification using the OARSI grading system [22] confirmed significant prevention of cartilage destruction by the C/EBPβ haploinsufficiency (Figure 6C).

Discussion

The present study for the first time demonstrated that the transcription factor C/EBPβ is essential for physiological skeletal growth and endochondral ossification by analyses of the deficient mice. This function was dependent on the promotion of transition from proliferation to hypertrophic differentiation of chondrocytes through the cell cycle control. Our further screening of cell cycle factors identified the cyclin-dependent kinase inhibitor p57 as the transcriptional target, and detected a responsive element of C/EBPβ in the promoter. We finally showed the functional mediation of p57 in the C/EBPβ action, and confirmed the importance of the C/EBPβ-p57 signal in the chondrocyte hypertrophy during skeletal growth and osteoarthritis progression.

Growth retardation of C/EBPβ−/− mice was seen during embryogenesis only and disappeared as the animals grew up after birth under physiological conditions (Figure 1A & B). This may possibly be due to compensatory mechanisms by other C/EBP family members which are known to control cellular differentiation in several lineages [23–26]. Regarding the mesenchymal cell lineage, C/EBPδ has been reported to show similar and compensatory actions for adipogenic and osteogenic differentiation [11,27–31]. Since the involvement of C/EBPδ in chondrogenic differentiation from the mesenchymal precursors remains unknown, we initially examined the expression by immunohistochemistry in the limb cartilage (E16.5) (Figure S1A). It was expressed predominantly in late proliferative and pre-hypertrophic chondrocytes, similarly to the C/EBPβ expression, and this was not altered in the C/EBPβ−/− cartilage. In addition, retroviral overexpression of C/EBPδ enhanced hypertrophic differentiation determined by COL10 and MMP13 mRNA levels in cultured ATDC5 cells (Figure S1B). Furthermore, the p57 promoter activity was enhanced by the C/EBPδ overexpression, although the effect was somewhat weaker than that by C/EBPβ (Figure S1C). Although we could not detect the distinct regulation of C/EBPβ and C/EBPδ expressions in the limb chondrocytes before and after birth, their actions on chondrocyte hypertrophy might be compensatory, especially postnatally. We are now investigating the role of C/EBPδ in the skeletal growth using the knockout mice as well as the double knockout mice of C/EBPβ and C/EBPδ.

The runt family transcription factor member Runx2 [1,32,33], parathyroid hormone/parathyroid hormone-related protein (PTH/PTHrP) [1,34], and cyclic GMP-dependent protein kinase II (cGKII) [35,36] are known as representative regulators of chondrocyte hypertrophy, and interestingly, C/EBPβ has been reported to be associated with these representative regulators. C/EBPβ acts as a co-activator of Runx2 [6,37]. Generally, the complex of the members of the C/EBP and Runx families is known to interact in the activation of lineage-specific promoters during differentiation of osteoblasts, adipocytes, and granulocytes [6]. Unlike Runx2−/− mice that exhibit a complete lack of bone [32], C/EBPβ−/− mice showed almost normal bone, raising the possibility of functional redundancy with other isoforms such as C/EBPα or C/EBPδ in osteoblast differentiation. Contrarily, both Runx2−/− and C/EBPβ−/− mice showed impairment of chondrocyte hypertrophy during cartilage development and growth [32,33], implicating a specific interaction between C/EBPβ and Runx2 in cartilage. In the present study, the site-directed mutagenesis in the C/EBP motif of the p57 promoter caused significant but incomplete suppression of the promoter activity induced by the C/EBPβ overexpression (Figure 5C). Actually, there is a putative Runx motif which lies close to this C/EBP motif in this region. C/EBPβ might therefore stimulate the promoter activity at the Runx motif as a co-activator of Runx2, even after the innate binding was blocked, although our luciferase assay and EMSA so far have failed to find evidence of this.

Contrarily to Runx2, PTH/PTHrP keeps chondrocytes proliferating and inhibits their hypertrophic differentiation [1,34]. The PTH/PTHrP action via the adenyl cyclase signal in chondrocytes is reported to be dependent on the suppression of p57 expression [38], implicating a possible mediation of C/EBPβ in this pathway. However, our present study showed that neither PTH nor the adenyl cyclase activator forskolin affected the C/EBPβ protein level in cultured ATDC5 cells or the activity of the p57 promoter (−150 to +226 bp) with or without induction by C/EBPβ (Figure S2). Although C/EBPβ is therefore unlikely to mediate the p57 suppression by PTH/PTHrP directly, its possible involvement as a co-activator of Runx2 again cannot be denied here, since the PTH/PTHrP action is also at least partly dependent on the Runx2 suppression in chondrocytes [39].

cGKII is a serine/threonine kinase lying downstream of the C-type natriuretic peptide pathway which is essential for skeletal growth [40]. We and others have reported that the deficiency of cGKII in mice and rats caused dwarfism due to impaired hypertrophic differentiation of chondrocytes [35,41], similarly to the present C/EBPβ−/− mice. Interestingly, a previous study showed that cGKII activated C/EBPβ through phosphorylation of glycogen synthase kinase-3β (GSK-3β) in osteosarcoma cells [42], and our recent study showed that cGKII induced chondrocyte hypertrophic differentiation through the GSK-3β phosphorylation [36]. These suggest a possible mediation of the present C/EBPβ-

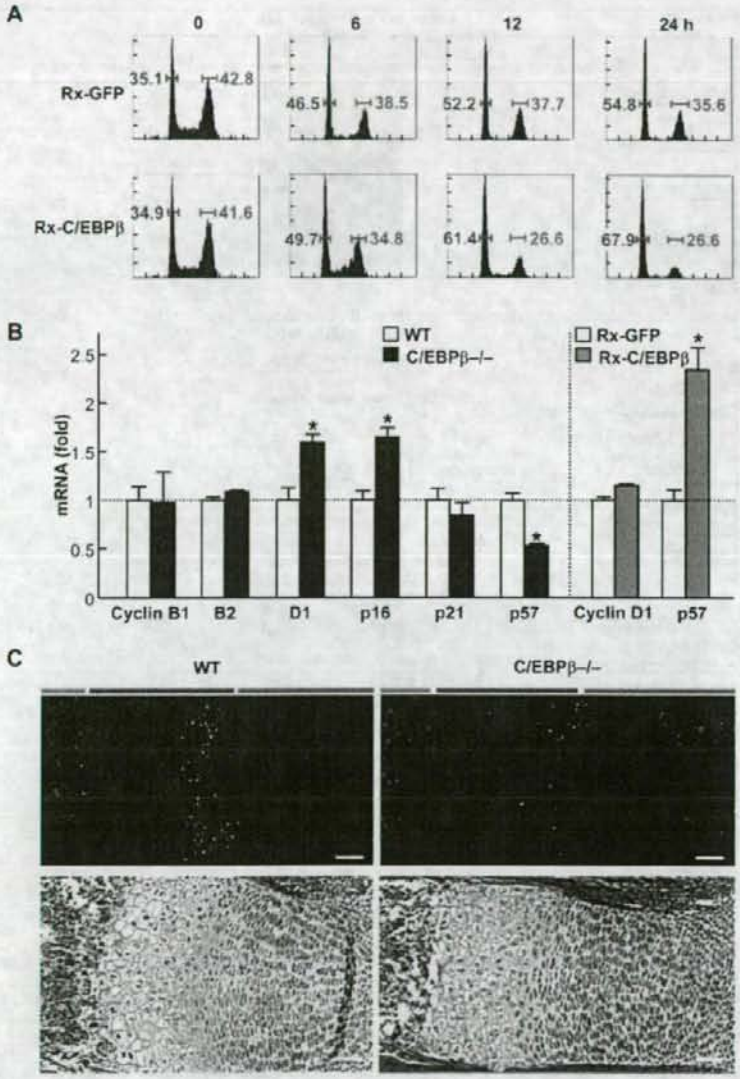

Figure 4. C/EBPβ affects cell cycle factors. (A) Time course of DNA histograms by a flow cytometric analysis of C3H10T1/2 cells with retroviral transfection of C/EBPβ (Rx-C/EBPβ) or the control GFP (Rx-GFP) after synchronization at the G2/M phase by nocodazole treatment. The horizontal and vertical axes represent the DNA content and relative frequency, respectively. The blue and red bars indicate the rates of cells in G0/G1 and G2/M phases, respectively. (B) Effects of loss- and gain-of-functions of C/EBPβ on relative mRNA levels of cell cycle factors that were identified as possible transcriptional targets of C/EBPβ by a microarray analysis (Table S1). The levels were compared by real-time RT-PCR analysis in the cultures between wild-type (WT) and C/EBPβ −/− rib chondrocytes (left), and between WT rib chondrocytes with Rx-C/EBPβ and Rx-GFP (right). Data are expressed as means (bars) ± SEM (error bars) of 6 samples per group. (C) Double immunofluorescence of p57 (green) and BrdU (red) in the proximal cartilage of tibias of the two genotype embryos (E16.5) and the HE staining (bottom) as a reference. Red, blue, and green bars indicate layers of proliferative zone, hypertrophic zone, and bone area, respectively. Scale bars, 50 μm.
doi:10.1371/journal.pone.0004543.g004

p57 signal in the cGKII-GSK-3β action. However, neither cGKII nor GSK-3β overexpression altered at least the activity of the p57 promoter (−150 to +226 bp) with or without induction by C/EBPβ (Figure S3). Moreover, there is a marked difference in the limb cartilage phenotype between cGKII−/− and C/EBPβ−/− mice. Unlike the cGKII−/− cartilage characterized by appearance of a wide abnormal intermediate layer between the proliferative and hypertrophic zones [35,41], the C/EBPβ−/−

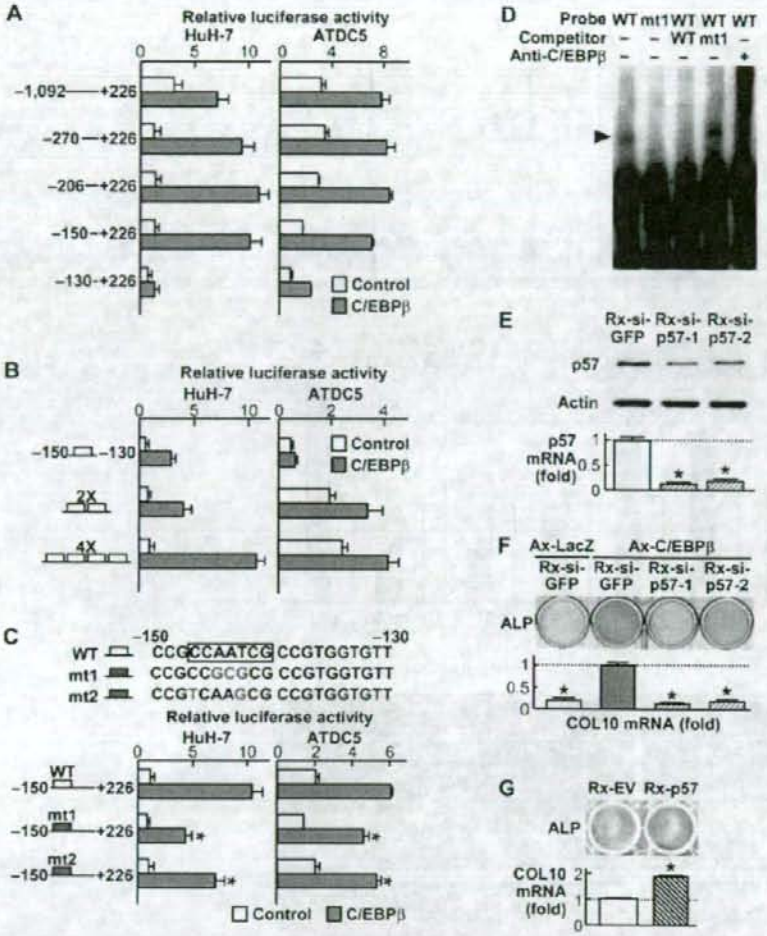

Figure 5. C/EBPβ transactivates p57 through binding to a C/EBP motif and the C/EBPβ-p57 signal induces chondrocyte hypertrophic differentiation. (A) Deletion analysis using luciferase-reporter constructs containing the 5′-flanking sequences from −1,092 to +226 bp of the p57 promoter and a series of deletion fragments in HuH-7 and ATDC5 cells transfected with C/EBPβ or the control GFP. (B) Dose-response analysis of the tandem repeats of the identified responsive element (−150/−130) by the luciferase-reporter assay in the HuH-7 and ATDC5 cells. (C) Site-directed mutagenesis analysis by two mutations (mt1 and mt2) in the C/EBPβ motif (−147/−141) as compared to the wild-type (WT) construct by the luciferase-reporter assay in HuH-7 and ATDC5 cells. *P<0.01 vs. WT-C/EBPβ. (D) EMSA for specific binding of the nuclear extract from C/EBPβ-transfected ATDC5 cells with the oligonucleotide probe (−160/−120) containing the WT or mt1 C/EBPβ motif. The arrowhead indicates the complex. Cold competition with 50-fold excess of unlabeled WT or mt1 probe, and supershift by an antibody to C/EBPβ of the complex are also presented. (E) The protein and mRNA levels of p57 determined by immunoblotting and real-time RT-PCR, respectively, by the p57 siRNA. Stable lines of C3H10T1/2 cells retrovirally transfected with two kinds of siRNA of p57 (Rx-si-p57-1 and Rx-si-p57-2) or the control GFP siRNA (Rx-si-GFP) were established. *P<0.01 vs. Rx-si-GFP. (F) Effects of the p57 siRNA above on the C/EBPβ-induced hypertrophic differentiation of chondrocytes. Primary rib chondrocytes were transfected with Rx-si-p57-1, Rx-si-p57-2, or Rx-si-GFP, and further adenovirally co-transfected with C/EBPβ or the control LacZ (Ax-C/EBPβ or Ax-LacZ). Hypertrophic differentiation was determined by ALP staining and relative COL10 mRNA level by real-time RT-PCR analysis at 2 weeks of culture after confluency. *P<0.01 vs. Ax-C/EBPβ with Rx-si-GFP. (G) Hypertrophic differentiation of ATDC5 cells stably transfected with the retrovirus expressing p57 (Rx-p57) or the empty vector (Rx-EV) cultured for 3 weeks with insulin and further for 2 d with inorganic phosphate. *P<0.01 vs. Rx-EV. All graphs are expressed as means (bars)±SEM (error bars) for 6 wells/group.
doi:10.1371/journal.pone.0004543.g005

cartilage only exhibited an elongated proliferative zone and delayed chondrocyte hypertrophy (Figure 2D). Hence, the cell cycle arrest in chondrocytes caused by C/EBPβ appears to immediately link to the start of the differentiation. The discrepancy may be due to the diversity of signaling pathway(s) lying downstream of cGKII and upstream of C/EBPβ. We previously reported that cGKII phosphorylated Sox9, an inhibitor of chondrocyte hypertrophy, and suppressed its nuclear entry [35]. Besides Sox9 and GSK-3β, vasodilator-stimulated phosphoprotein and cysteine- and glycine-rich protein 2 are putative phosphor-

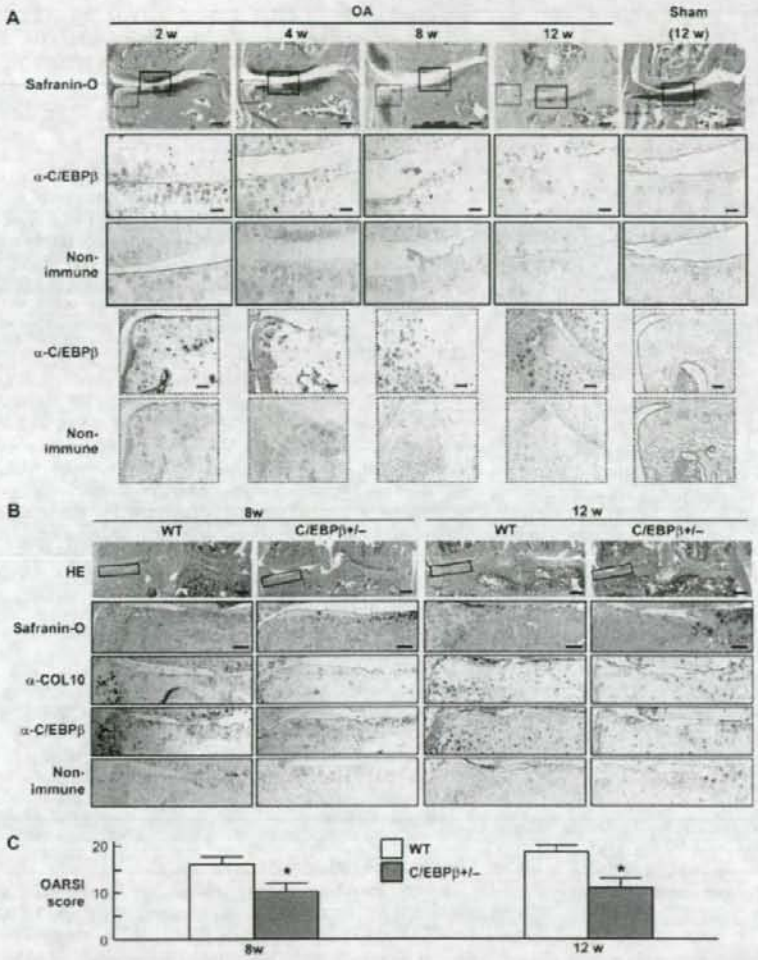

Figure 6. C/EBPβ is involved in cartilage destruction during osteoarthritis progression. (A) Time course of joint cartilage destruction and C/EBPβ expression in the medial portion of cartilage after creating an experimental osteoarthritis model that induces instability to the knee joints of 8-week-old wild-type mice. Safranin-O staining and immunohistochemical staining with an antibody to C/EBPβ (α-C/EBPβ) or the non-immune control IgG were performed at the indicated weeks after surgery. A sham operation was performed using the same approach, and assessed after 12 weeks. Boxed areas with solid and dotted lines in the top row indicate the regions of the other rows. Scale bars, 100 μm (top) and 400 μm (others). (B) HE and Safranin-O stainings, and immunohistochemical stainings with α-C/EBPβ and α-COL10 or the non-immune IgG in the tibial cartilage of wild-type (WT) and C/EBPβ+/− littermates 8 weeks and 12 weeks after the surgery. Boxed areas in the top row indicate the regions of the other rows. Scale bars, 200 μm (top), 400 μm (others). (C) Cartilage destruction according to the OARSI grading system. Data are expressed as means (bars) ± SEM (error bars) for 5 mice per genotype at 8 and 12 weeks. *$P<0.05$ vs. WT
doi:10.1371/journal.pone.0004543.g006

ylation targets of cGKII in other types of cells [43]. In addition to the abovementioned GSK-3β, C/EBPβ is also targeted by multiple protein kinases including protein kinase A, calmodulin-dependent protein kinase, Erk-1/2, ribosomal protein S6 kinase, and CDK2 [44].

The skeletal abnormalities of C/EBPβ−/− mice were much milder than those of the p57−/− mice which were perinatally lethal due to various defects analogous to Beckwith-Weidemann syndrome in children, including cleft palate and body wall dysplasia besides severe dwarfism [38,45–47]. This may be because p57 is more crucial for chondrocyte hypertrophic differentiation than C/EBPβ whose function could be substituted by several upstream signals of p57. In fact, the C/EBPβ deficiency did not abrogate, but partially suppressed the p57 expression in chondrocytes (Figure 4B, C), while the knockdown of p57 strongly suppressed the C/EBPβ-induced hypertrophic differentiation of chondrocytes (Figure 5F). Among other cell cycle factors, mice lacking the Rb-related pocket proteins p107 and p130 show skeletal phenotype very similar to that of the p57−/− mice [48], indicating that these proteins are likely to be major downstream

targets of the cyclin-CDK complexes that are inhibited by p57 in chondrocytes. More interestingly, the Cip/Kip family proteins have recently been reported to regulate pathways distinct from that of cell cycle control [14]. Since p57 supports skeletal myoblast differentiation by inhibiting phosphorylation of the key transcription factor MyoD [49], this factor might also induce chondrocyte hypertrophic differentiation by regulating crucial transcription factors like Runx2 or Sox9. This may also explain the direct linkage from the cell cycle arrest to cell differentiation by the C/EBPβ-p57 signaling, unlike the cGKII signal, as mentioned above.

We conclude that C/EBPβ directly transactivates p57 to promote transition from proliferation to hypertrophic differentiation of chondrocytes during endochondral ossification. Besides the anabolic function for physiological skeletal growth, the C/EBPβ haploinsufficiency in adult mice caused resistance to cartilage destruction during osteoarthritis progression in knee joints (Figure 6). Furthermore, C/EBPβ has been reported to be induced by proinflammatory cytokines interleukin-1 and tumor necrosis factor-α, and to mediate the decrease of articular cartilage matrix by suppressing the promoter activity of cartilage characteristic genes like cartilage-derived retinoic acid-sensitive protein and type II collagen [50–52]. The cytokine-induced C/EBPβ also enhances the promoter activity of prostaglandin synthetic enzymes like cyclooxygenase-2 and phospholipase A2 [53,54] and proteinases like aggrecanase-1 and matrix metalloproteinase-1 [55,56] in chondrocytes. These lines of evidence indicate that the C/EBPβ-p57 signal could be a therapeutic target of inflammatory and degenerative joint disorders as well as skeletal growth retardation.

Materials and Methods

Ethics statement

All experiments were performed according to the protocol approved by the Animal Care and Use Committee of the University of Tokyo.

Animals

C/EBPβ deficient mice, kindly provided by Dr. Shizuo Akira (University of Osaka), were maintained in a C57BL/6 background. In each experiment, we compared C/EBPβ−/− or C/EBPβ+/− mice with the wild-type littermates.

Histological analysis

The whole skeletons of WT and C/EBPβ−/− littermate embryos (E16.5) were fixed in 99.5% ethanol, transferred to acetone, and stained in a solution containing Alizarin red S and Alcian blue 8GX (Sigma). For histological analysis, tibial limbs were fixed in 4% paraformaldehyde (PFA) buffered with PBS and sectioned in 5-μm slices. Hematoxylin-eosin (HE) stainings were performed according to standard protocols. Alcian blue/von Kossa double stainings were performed with 1% Alcian blue 8GX in 3% acetate and with 5% silver nitrate. For immunohistochemistry, the sections were incubated with antibodies to C/EBPβ (C-19), p57 (C-20), Ihh (C-15), and C/EBPδ (M-17) (Santa Cruz Biotechnology Inc.) diluted 1:500 in blocking reagent. The localization of C/EBPβ was detected with HRP-conjugated secondary antibody (Promega). For fluorescent visualization, a secondary antibody conjugated with Alexa Fluor 488 (Invitrogen) was used. The p57 detection was performed using a CSA II, Biotin-Free Catalyzed Amplification System (DAKO). In situ hybridization was performed, as we reported previously [21]. Briefly, hybridization with complementary digoxigenin (DIG)-labeled for mouse type X collagen was performed in a humidified chamber for 16 h at 52°C. For the detection of DIG-labeled probes, slides were incubated with HRP-conjugated anti-DIG rabbit polyclonal antibody (Dakopatts). The sections were immersed in a diaminobenzidine solution to visualize immunoreactivity. For BrdU labeling, we injected BrdU (Sigma) intraperitoneally to pregnant mice prior to sacrifice, and the sections were stained using a BrdU Immunohistochemistry System (Calbiochem) and Alexa Fluor 568 (Molecular Probes).

Cell cultures

Primary chondrocytes were isolated from the ribs of mouse embryos as previously described [57]. The primary chondrocytes, HuH-7 cells and C3H10T1/2 cells were cultured in DMEM with 10% FBS. ATDC5 cells were maintained in DMEM/F12 with 5% FBS. To induce hypertrophic differentiation, the ATDC5 cells were cultured for 3 weeks with insulin.

Plasmids and viral vectors

C/EBPβ and p57 cDNA were cloned into pMx vectors, and retroviral vectors were generated using plat-E cells [58]. The siRNA sequence was designed for the mouse p57 gene (NM_009876.3: nucleotides 925–946 and 307–328) and GFP as previously described [59] and ligated into piGENEmU6 vector (iGENE Therapeutics). The siRNA sequence combined with the promoter was then inserted into a retroviral pMx vector. The adenovirus C/EBPβ and LacZ expression vector were synthesized using an Adeno-X expression system (Clontech). Two weeks after transfection, the cells were harvested and used for subsequent assays. cDNA of cGKII and GSK-3β was ligated into pCMV-HA (Invitrogen).

Cell proliferation assay

Primary chondrocytes were inoculated at 10^3 cells per well in a 96-well plate. The proliferation of cells was examined, using an XTT Assay Kit (Roche) at the indicated time point. The absorbance of the product was quantified using a MTP-300 microplate reader (Corona Electric). For BrdU detection analysis, we labeled the chondrocytes with 10 μM BrdU (Sigma) for 18 h and the cells were stained using a BrdU Immunohistochemistry System (Calbiochem).

Chondrocyte differentiation assay

Primary chondrocytes were cultured for two weeks after confluency, and the total RNA was extracted to assess the COL10, MMP13, and VEGF mRNA levels. For the ALP staining, cells were stained with a solution containing 0.01% Naphthol AS-MX phosphate disodium salt (Sigma), 1% N, N-dimethyl-formamide (Wako), and 0.06% fast blue BB (Sigma). For the Alizarin red S staining, cells were stained with 2% Alizarin red S solution (Sigma).

Flow cytometric analysis

C3H10T1/2 cells with retroviral transfection with C/EBPβ or GFP were incubated for 18 h in the presence of 0.2 μM nocodazole for synchronization at the G2/M phase. Then, cells were suspended in citrate buffer and stained with propidium iodide. DNA content was analyzed with EPICS XL and XL EXPO32 instruments (Beckman).

Real-time RT-PCR

The total RNA was extracted using an ISOGEN Kit (Wako) and an RNeasy Mini Kit (QIAGEN). One μg of RNA was reverse-transcribed with a Takara RNA PCR Kit (AMV) ver.2.1 (Takara) to generate single-stranded cDNA. PCR was performed with an ABI Prism 7000 Sequence Detection System (Applied Biosystems). All reactions were run in triplicate. Primer sequence information is available upon request.

Luciferase assay

The human p57 promoter regions were cloned into the pGL4.10 vector (Promega). Other deletion constructs were created by the PCR technique. Tandem-repeat constructs were created by ligating the double strand oligonucleotides from −150 to −130 bp into pGL4.10 vector. Transfection in HuH-7 and ATDC5 cells was performed in quadruplicate using Fugene (Roche). For PTH or forskolin stimulation, cells were cultured with PTH (10 nM) or forskolin (10 nM) at the time of transfection. The luciferase assay was performed with a PicaGene Dual SeaPansy Luminescence Kit (Toyo Ink) and GloMax™ 96 Microplate Luminometer (Promega).

Electrophoretic Mobility Shift Assay (EMSA)

Nuclear extracts were prepared from ATDC5 cells adenovirally transfected with C/EBPβ. Oligonucleotide probes of the −160 to −120 bp region sequence in the p57 promoter were labeled with digoxigenin by using a DIG gel shift kit (Roche). For competition analyses, 50-fold excess of unlabeled competitor probe was included in the binding reaction. For the supershift experiments, 1 μL of an antibody to C/EBPβ (Santa Cruz Biotechnology Inc.) was added.

Microarray analysis

Total RNA was isolated from C3H10T1/2 cells with retroviral introduction of C/EBPβ or the empty vector after 1 week of culture. The microarray experiment was performed using the Gene Chip Mouse Genome 430 2.0 Array (Affymetrix), scanned by GeneChip Scanner 3000, and analyzed using GCOS ver 1.4 software.

Immunoblotting

ATDC5 cells were cultured with PTH (10 nM) or forskolin (10 nM) for 0 to 30 min, and then their cytoplasmic and nuclear proteins were extracted with an NE-PER (Pierce Chemical). For immunoblot analysis, lysates were fractionated by SDS-PAGE and transferred onto nitrocellulose membranes (BIO-RAD). The membranes were incubated with an antibody to C/EBPβ (Santa Cruz), or an antibody to actin (Sigma). Immunoreactive bands were visualized with ECL Plus (Amersham Biosciences).

Osteoarthritis experiment

The surgical procedure to create an osteoarthritis experimental model was performed on 8-week-old male mice, as we have reported previously [17,20,21]. At the indicated time points after surgery, the mice were killed, and the entire knee joints were dissected and fixed for 24 h at 4°C in 4% PFA. The specimens were decalcified for 2 weeks with 10% EDTA (pH 7.4) at 4°C and sectioned in 5-μm slices. Sections were stained with Safranin O fast green. Destruction of cartilage was quantified according to the OARSI grading system [22]. For immunohistochemistry, the sections were incubated with antibodies to C/EBPβ (Santa Cruz), COL10 (LSL) or the nonimmune rabbit IgG as the negative control diluted 1:500 in blocking reagent, and the localization was detected with HRP-conjugated secondary antibody (Promega).

Statistical analysis

Means of groups were compared by ANOVA, and significance of differences was determined by post-hoc testing using Bonferroni's method.

Supporting Information

Table S1 Microarray analysis shows the changes in expression of cell cycle factors by C/EBPβ overexpression. Ratios of mRNA levels in C3H10T1/2 cells with retroviral introduction of C/EBPβ in comparison with the control empty vector were determined by Gene Chip Mouse Genome 430 2.0 Array (Affymetrix). All results of the microarray analysis are provided at ArrayExpress (accession number: E-MEXP-1984).
Found at: doi:10.1371/journal.pone.0004543.s001 (0.02 MB PDF)

Figure S1 C/EBPδ shows similar expression and function in chondrocytes to those of C/EBPβ. (A) Immunostaining with an antibody to C/EBPδ in the tibial cartilage of wild-type (WT) and C/EBPβ−/− littermates (E16.5). Red, blue, and green bars indicate layers of proliferative zone, hypertrophic zone, and bone area, respectively. Scale bars, 100 mm. (B) Relative mRNA levels of COL10, MMP13, and VEGF of ATDC5 cells with retroviral transfection of C/EBPδ or the control GFP determined by real-time RT-PCR at 2 weeks of culture after confluency. (C) The p57 promoter activity in ATDC5 cells transfected with luciferase-reporter construct containing the 5′-flanking sequences from −150 to +226 bp of the p57 promoter with effector plasmid expressing C/EBPδ, C/EBPβ, or the control GFP. All data are expressed as means (symbols or bars) ± SEM (error bars) of 6 wells per group. *P<0.01 vs. GFP.
Found at: doi:10.1371/journal.pone.0004543.s002 (0.68 MB PDF)

Figure S2 PTH and forskolin have no effects on C/EBPβ protein level and p57 promoter activity. (A) Time course of C/EBPβ protein level in cultured ATDC5 cells. After the indicated time of treatment with PTH (10 nM) and forskolin (10 nM), the C/EBPβ protein levels in the cytoplasmic fraction (C) and nuclear fraction (N) were determined by immunoblotting with an antibody to C/EBPβ or actin as the loading control. (B) Effects of PTH, forskolin or the control on HuH-7 cells transfected with luciferase-reporter construct containing the 5′-flanking fragment (−150 to +226 bp) of the p57 promoter with effector plasmid expressing C/EBPβ or GFP as the control. The promoter activity was determined by the luciferase assay after 2 d of treatment.
Found at: doi:10.1371/journal.pone.0004543.s003 (0.07 MB PDF)

Figure S3 Effects of cGKII and GSK-3β overexpression on p57 promoter activity. The promoter activity was determined by the luciferase assay in HuH-7 cells transfected with luciferase-reporter construct containing the 5′-flanking fragment (−150 to +226 bp) of the p57 promoter with effector plasmid expressing C/EBPβ or GFP as the control.
Found at: doi:10.1371/journal.pone.0004543.s004 (0.02 MB PDF)

Author Contributions

Conceived and designed the experiments: MH FK TI KN UiC HK. Performed the experiments: MH FK AF SO TO. Analyzed the data: MH FK AF. Contributed reagents/materials/analysis tools: SO NK TO YK TS FY TI UiC. Wrote the paper: MH NK HK.

References

1. Kronenberg HM (2003) Developmental regulation of the growth plate. Nature 423: 332–336.

2. Hunziker EB (1994) Mechanism of longitudinal bone growth and its regulation by growth plate chondrocytes. Microsc Res Tech 28: 505–519.

3. Wilsman NJ, Farnum CE, Leiferman EM, Fry M, Barreto C (1996) Differential growth by growth plates as a function of multiple parameters of chondrocytic kinetics. J Orthop Res 14: 927–936.
4. Descombes P, Chojkier M, Lichtsteiner S, Falvey E, Schibler U (1990) LAP, a novel member of the C/EBP gene family, encodes a liver-enriched transcriptional activator protein. Genes Dev 4: 1541–1551.
5. Landschulz WH, Johnson PF, Adashi EY, Graves BJ, McKnight SL (1988) Isolation of a recombinant copy of the gene encoding C/EBP. Genes Dev 2: 786–800.
6. Nerlov C (2007) The C/EBP family of transcription factors: a paradigm for interaction between gene expression and proliferation control. Trends Cell Biol 17: 318–324.
7. Johnson PF (2005) Molecular stop signs: regulation of cell-cycle arrest by C/EBP transcription factors. J Cell Sci 118: 2545–2555.
8. Wu Z, Xie Y, Bucher NL, Farmer SR (1995) Conditional ectopic expression of C/EBP beta in NIH-3T3 cells induces PPAR gamma and stimulates adipogenesis. Genes Dev 9: 2350–2363.
9. Screpanti I, Romani L, Musiani P, Modesti A, Fattori E, et al. (1995) Lymphoproliferative disorder and imbalanced T-helper response in C/EBP beta-deficient mice. EMBO J 14: 1932–1941.
10. Tanaka T, Akira S, Yoshida K, Umemoto M, Yoneda Y, et al. (1995) Targeted disruption of the NF-IL6 gene discloses its essential role in bacteria killing and tumor cytotoxicity by macrophages. Cell 80: 353–361.
11. Tanaka T, Yoshida N, Kishimoto T, Akira S (1997) Defective adipocyte differentiation in mice lacking the C/EBPbeta and/or C/EBPdelta gene. EMBO J 16: 7432–7443.
12. LuValle P, Beier F (2000) Cell cycle control in growth plate chondrocytes. Front Biosci 5: D493–503.
13. Moro T, Ogasawara T, Chikuda H, Ikeda T, Ogata N, et al. (2005) Inhibition of Cdk6 expression through p38 MAP kinase is involved in differentiation of mouse prechondrocyte ATDC5. J Cell Physiol 204: 927–933.
14. Besson A, Dowdy SF, Roberts JM (2008) CDK inhibitors: cell cycle regulators and beyond. Dev Cell 14: 159–169.
15. Meergans T, Albig W, Doenecke D (1998) Conserved sequence elements in human main type-H1 histone gene promoters: their role in H1 gene expression. Eur J Biochem 256: 436–446.
16. Drissi H, Zuscik M, Rosier R, O'Keefe R (2005) Transcriptional regulation of chondrocyte maturation: potential involvement of transcription factors in OA pathogenesis. Mol Aspects Med 26: 169–179.
17. Kamekura S, Kawasaki Y, Hoshi K, Shimoaka T, Chikuda H, et al. (2006) Contribution of runt-related transcription factor 2 to the pathogenesis of osteoarthritis in mice after induction of knee joint instability. Arthritis Rheum 54: 2462–2470.
18. Kawaguchi H (2008) Endochondral ossification signals in cartilage degradation during osteoarthritis progression in experimental mouse models. Mol Cells 25: 1–6.
19. Kuhn K, D'Lima DD, Hashimoto S, Lotz M (2004) Cell death in cartilage. Osteoarthritis Cartilage 12: 1–16.
20. Yamada T, Kawano H, Koshizuka Y, Fukuda T, Yoshimura K, et al. (2006) Carminerin contributes to chondrocyte calcification during endochondral ossification. Nat Med 12: 665–670.
21. Kamekura S, Hoshi K, Shimoaka T, Chung U, Chikuda H, et al. (2005) Osteoarthritis development in novel experimental mouse models induced by knee joint instability. Osteoarthritis Cartilage 13: 632–641.
22. Pritzker KP, Gay S, Jimenez SA, Ostergaard K, Pelletier JP, et al. (2006) Osteoarthritis cartilage histopathology: grading and staging. Osteoarthritis Cartilage 14: 13–29.
23. Darlington GJ (1999) Molecular mechanisms of liver development and differentiation. Curr Opin Cell Biol 11: 678–682.
24. Darlington GJ, Ross SE, MacDougald OA (1998) The role of C/EBP genes in adipocyte differentiation. J Biol Chem 273: 30057–30060.
25. Radomska HS, Huettner CS, Zhang P, Cheng T, Scadden DT, et al. (1998) CCAAT/enhancer binding protein alpha is a regulatory switch sufficient for induction of granulocytic development from bipotential myeloid progenitors. Mol Cell Biol 18: 4301–4314.
26. Zhang DE, Hetherington CJ, Meyers S, Rhoades KL, Larson CJ, et al. (1996) CCAAT enhancer-binding protein (C/EBP) and AML1 (CBF alpha2) synergistically activate the macrophage colony-stimulating factor receptor promoter. Mol Cell Biol 16: 1231–1240.
27. Cao Z, Umek RM, McKnight SL (1991) Regulated expression of three C/EBP isoforms during adipose conversion of 3T3-L1 cells. Genes Dev 5: 1538–1552.
28. Gutierrez S, Javed A, Tennant DK, van Rees M, Montecino M, et al. (2002) CCAAT/enhancer-binding proteins (C/EBP) beta and delta activate osteocalcin gene transcription and synergize with Runx2 at the C/EBP element to regulate bone-specific expression. J Biol Chem 277: 1316–1323.
29. Lin FT, Lane MD (1992) Antisense CCAAT/enhancer-binding protein RNA suppresses coordinate gene expression and triglyceride accumulation during differentiation of 3T3-L1 preadipocytes. Genes Dev 6: 533–544.
30. Lin FT, Lane MD (1994) CCAAT/enhancer binding protein alpha is sufficient to initiate the 3T3-L1 adipocyte differentiation program. Proc Natl Acad Sci U S A 91: 8757–8761.
31. Yeh WC, Cao Z, Classon M, McKnight SL (1995) Cascade regulation of terminal adipocyte differentiation by three members of the C/EBP family of leucine zipper proteins. Genes Dev 9: 168–181.
32. Komori T (2005) Regulation of skeletal development by the Runx family of transcription factors. J Cell Biochem 95: 445–453.
33. Takeda S, Bonnamy JP, Owen MJ, Ducy P, Karsenty G (2001) Continuous expression of Cbfa1 in nonhypertrophic chondrocytes uncovers its ability to induce hypertrophic chondrocyte differentiation and partially rescues Cbfa1-deficient mice. Genes Dev 15: 467–481.
34. Kronenberg HM (2006) PTHrP and skeletal development. Ann N Y Acad Sci 1068: 1–13.
35. Chikuda H, Kugimiya F, Hoshi K, Ikeda T, Ogasawara T, et al. (2004) Cyclic GMP-dependent protein kinase II is a molecular switch from proliferation to hypertrophic differentiation of chondrocytes. Genes Dev 18: 2418–2429.
36. Kawasaki Y, Kugimiya F, Chikuda H, Kamekura S, Ikeda T, et al. (2008) Phosphorylation of GSK-3beta by cGMP-dependent protein kinase II promotes hypertrophic differentiation of murine chondrocytes. J Clin Invest 118: 2506–2515.
37. Hata K, Nishimura R, Ueda M, Ikeda F, Matsubara T, et al. (2005) A CCAAT/enhancer binding protein beta isoform, liver-enriched inhibitory protein, regulates commitment of osteoblasts and adipocytes. Mol Cell Biol 25: 1971–1979.
38. MacLean HE, Guo J, Knight MC, Zhang P, Cobrinik D, et al. (2004) The cyclin-dependent kinase inhibitor p57(Kip2) mediates proliferative actions of PTHrP in chondrocytes. J Clin Invest 113: 1334–1343.
39. Guo J, Chung UI, Yang D, Karsenty G, Bringhurst FR, et al. (2006) PTH/PTHrP receptor delays chondrocyte hypertrophy via both Runx2-dependent and -independent pathways. Dev Biol 292: 116–128.
40. Pejchalova K, Krejci P, Wilcox WR (2007) C-natriuretic peptide: an important regulator of cartilage. Mol Genet Metab 92: 210–215.
41. Pfeifer A, Aszodi A, Seidler U, Ruth P, Hofmann F, et al. (1996) Intestinal secretory defects and dwarfism in mice lacking cGMP-dependent protein kinase II. Science 274: 2082–2086.
42. Zhao X, Zhuang S, Chen Y, Boss GR, Pilz RB (2003) Cyclic GMP-dependent protein kinase regulates CCAAT enhancer-binding protein beta function through inhibition of glycogen synthase kinase-3. J Biol Chem 280: 32683–32692.
43. Schlossmann J, Hofmann F (2005) cGMP-dependent protein kinases in drug discovery. Drug Discov Today 10: 627–634.
44. Li H, Gade P, Xiao W, Kalvakolanu DV (2007) The interferon signaling network and transcription factor C/EBP-beta. Cell Mol Immunol 4: 407–418.
45. Takahashi K, Nakayama K, Nakayama K (2000) Mice lacking a CDK inhibitor, p57Kip2, exhibit skeletal abnormalities and growth retardation. J Biochem 127: 73–83.
46. Yan Y, Frisen J, Lee MH, Massague J, Barbacid M (1997) Ablation of the CDK inhibitor p57Kip2 results in increased apoptosis and delayed differentiation during mouse development. Genes Dev 11: 973–983.
47. Zhang P, Liegeois NJ, Wong C, Finegold M, Hou H, et al. (1997) Altered cell differentiation and proliferation in mice lacking p57KIP2 indicates a role in Beckwith-Wiedemann syndrome. Nature 387: 151–158.
48. Rossi F, MacLean HE, Yuan W, Francis RO, Semenova E, et al. (2002) p107 and p130 Coordinately regulate proliferation, Cbfa1 expression, and hypertrophic differentiation during endochondral bone development. Dev Biol 247: 271–285.
49. Reynaud EG, Pripel K, Guillier M, Leibovitch MP, Leibovitch SA (1999) p57(Kip2) stabilizes the MyoD protein by inhibiting cyclin E-Cdk2 kinase activity in growing myoblasts. Mol Cell Biol 19: 7621–7629.
50. Imamura T, Imamura C, Iwamoto Y, Sandell LJ (2005) Transcriptional co-activators CREB-binding protein/p300 increase chondrocyte Cdi-cap gene expression by multiple mechanisms including sequestration of the repressor CCAAT/enhancer-binding protein. J Biol Chem 280: 16625–16634.
51. Imamura T, Imamura C, McAlinden A, Davies SR, Iwamoto Y, et al. (2008) A novel tumor necrosis factor alpha-responsive CCAAT/enhancer binding protein site regulates expression of the cartilage-derived retinoic acid-sensitive protein gene in cartilage. Arthritis Rheum 58: 1366–1376.
52. Okatsuka K, Yu H, Davies SR, Imamura T, Sandell LJ (2006) A promoter element of the CD-RAP gene is required for repression of gene expression in non-cartilage tissues in vitro and in vivo. J Cell Biochem 97: 857–868.
53. Massaad C, Paradon M, Jacques C, Sakut C, Berenbaum F, et al. (2000) Induction of secreted type IIA phospholipase A2 gene transcription by interleukin-1beta. Role of C/EBP factors. J Biol Chem 275: 22686–22694.
54. Thomas B, Berenbaum F, Humbert L, Bian H, Bereziat G, et al. (2000) Critical role of C/EBPdelta and C/EBPbeta factors in the stimulation of the cyclooxygenase-2 gene transcription by interleukin-1beta in articular chondrocytes. Eur J Biochem 267: 6798–6809.
55. Mizui Y, Yamazaki K, Kohno Y, Sagane K, Tanaka I (2000) Characterization of 5'-flanking region of human aggrecanase-1 (ADAMTS4) gene. Mol Biol Rep 27: 167–173.
56. Raymond L, Eck S, Mollmark J, Hays E, Tomek I, et al. (2006) Interleukin-1 beta induction of matrix metalloproteinase-1 transcription in chondrocytes requires ERK-dependent activation of CCAAT enhancer-binding protein-beta. J Cell Physiol 207: 683–688.

57. Yano F, Kugimiya F, Ohba S, Ikeda T, Chikuda H, et al. (2005) The canonical Wnt signaling pathway promotes chondrocyte differentiation in a Sox9-dependent manner. Biochem Biophys Res Commun 333: 1300–1308.
58. Morita S, Kojima T, Kitamura T (2000) Plat-E: an efficient and stable system for transient packaging of retroviruses. Gene Ther 7: 1063–1066.
59. Kawasaki H, Taira K (2003) Short hairpin type of dsRNAs that are controlled by tRNA(Val) promoter significantly induce RNAi-mediated gene silencing in the cytoplasm of human cells. Nucleic Acids Res 31: 700–707.

ARTHRITIS & RHEUMATISM
Vol. 60, No. 1, January 2009, pp 166–178
DOI 10.1002/art.24243

Identification of the Core Element Responsive to Runt-Related Transcription Factor 2 in the Promoter of Human Type X Collagen Gene

Akiro Higashikawa, Taku Saito, Toshiyuki Ikeda, Satoru Kamekura, Naohiro Kawamura, Akinori Kan, Yasushi Oshima, Shinsuke Ohba, Naoshi Ogata, Katsushi Takeshita, Kozo Nakamura, Ung-il Chung, and Hiroshi Kawaguchi

Objective. **Type X collagen and runt-related transcription factor 2 (RUNX-2) are known to be important for chondrocyte hypertrophy during skeletal growth and repair and development of osteoarthritis (OA) in mice. Aiming at clinical application, this study was undertaken to investigate transcriptional regulation of human type X collagen by RUNX-2 in human cells.**

Methods. **Localization of type X collagen and RUNX-2 was determined by immunohistochemistry, and their functional interaction was examined in cultured mouse chondrogenic ATDC-5 cells. Promoter activity of the human type X collagen gene (COL10A1) was examined in human HeLa, HuH7, and OUMS27 cells transfected with a luciferase gene containing a 4.5-kb promoter and fragments. Binding to RUNX-2 was examined by electrophoretic mobility shift assay and chromatin immunoprecipitation.**

Results. **RUNX-2 and type X collagen were colocalized in mouse limb cartilage and bone fracture callus. Gain and loss of function of RUNX-2 revealed that RUNX-2 is essential for type X collagen expression and terminal differentiation of chondrocytes. Human COL10A1 promoter activity was enhanced by RUNX-2 alone and more potently by RUNX-2 in combination with the coactivator core-binding factor β in all 3 human cell lines examined. Deletion, mutagenesis, and tandem repeat analyses identified the core responsive element as the region between −89 and −60 bp (termed the hypertrophy box [HY box]), which showed specific binding to RUNX-2. Other putative RUNX-2 binding motifs in the human COL10A1 promoter did not respond to RUNX-2 in human cells.**

Conclusion. **Our findings indicate that the HY box is the core element responsive to RUNX-2 in human COL10A1 promoter. Studies on molecular networks related to RUNX-2 and the HY box will lead to treatments of skeletal growth retardation, bone fracture, and OA.**

Hypertrophic differentiation of chondrocytes during endochondral ossification is an essential step in skeletal growth and repair (1,2). We and others have reported that chondrocyte hypertrophy also contributes to cartilage degradation during the development of osteoarthritis (OA) (3–5). Type X collagen is a short, network-forming collagen specifically expressed by hypertrophic chondrocytes (6). The physiologic importance of type X collagen has been shown by the impairment of endochondral ossification and skeletal growth that results from loss of function of the type X collagen gene in mice (7–9). Similarly, mutations in the carboxy-terminal domain of the human type X collagen gene (COL10A1) cause a severe skeletal disorder called Schmid-type metaphyseal chondrodysplasia, with growth retardation, waddling gait, and OA (10–12). Hence, elucidation of the mechanisms regulating the type X collagen gene will contribute to understanding the molecular backgrounds of skeletal growth and repair and OA not only in mice, but also in humans.

Supported by a Grant-in-Aid for Scientific Research from the Japanese Ministry of Education, Culture, Sports, Science, and Technology (18659435).

Akiro Higashikawa, MD, Taku Saito, MD, PhD, Toshiyuki Ikeda, MD, Satoru Kamekura, MD, PhD, Naohiro Kawamura, MD, PhD, Akinori Kan, MD, Yasushi Oshima, MD, PhD, Shinsuke Ohba, PhD, Naoshi Ogata, MD, PhD, Katsushi Takeshita, MD, PhD, Kozo Nakamura, MD, PhD, Ung-il Chung, MD, PhD, Hiroshi Kawaguchi, MD, PhD: University of Tokyo, Tokyo, Japan.

Address correspondence and reprint requests to Hiroshi Kawaguchi, MD, PhD, Sensory and Motor System Medicine, Faculty of Medicine, University of Tokyo, Hongo 7-3-1, Bunkyo, Tokyo 113-8655, Japan. E-mail: kawaguchi-ort@h.u-tokyo.ac.jp.

Submitted for publication August 9, 2008; accepted in revised form October 13, 2008.

The specificity of type X collagen expression in hypertrophic chondrocytes underlies tight control by transcriptional regulation of gene expression. Runt-related transcription factor 2 (RUNX-2) was originally isolated on the basis of its ability to transactivate the osteoblast-specific osteocalcin gene and is well known as a key molecule for bone formation (13,14). However, recent in vivo studies in mice have revealed that RUNX-2 is the pivotal transcription factor for type X collagen expression and chondrocyte hypertrophy during endochondral ossification (15–20). RUNX-2 is known to function by forming a heterodimer with a cotranscription factor called core-binding factor β (CBFβ) (21).

In a previous study (22,23), we created an experimental OA model by induction of joint instability in mouse knee joints (5). RUNX-2 expression was induced in articular cartilage chondrocytes, followed by type X collagen expression and chondrocyte hypertrophy. Type X collagen expression and cartilage degradation were greatly suppressed in the joints of heterozygous *Runx2*-knockout (Runx2$^{+/-}$) mice as compared with their wild-type littermates. These findings indicate that the RUNX-2–type X collagen signal is likely to play a crucial role in pathologic skeletal disorders, such as OA, as well as in physiologic skeletal growth and repair. Although RUNX-2 has been reported to activate the promoter of the mouse Col10a1 gene directly via its putative RUNX-2 binding motifs (20), the mechanism of transcriptional regulation of the human COL10A1 gene by RUNX-2 remains unknown. Hence, aiming at clinical application of this signal to treatments of skeletal growth retardation, bone fracture, and OA, in this study we investigated the mechanism underlying the transcriptional regulation of human COL10A1 by RUNX-2 in human cells.

MATERIALS AND METHODS

Animals. All experiments were performed according to a protocol approved by the Animal Care and Use Committee of the University of Tokyo. Wild-type and heterozygous *Runx2*-deficient mice with the *lacZ* gene inserted at the site of the *Runx2* gene deletion (Runx2$^{+/\Delta lacZ}$) were maintained on a C57BL/6 background and were fed a standard rodent diet (CE-2; Clea, Tokyo, Japan).

Bone fracture experiment. A transverse osteotomy was created using a bone saw at the midshaft in the left femur of 8-week-old male Runx2$^{+/\Delta lacZ}$ mice, and was internally stabilized with an intramedullary nail using the inner pin of a 22-gauge spinal needle, as previously described (24–26). For histologic analyses, animals were killed by CO_2 asphyxiation 9 days after surgery, and femurs were excised.

Histologic analysis. Excised tibial limbs and femurs were fixed in 4% formaldehyde buffered with phosphate buffered saline (pH 7.4) for 1 hour at 4°C and rinsed 3 times with washing buffer (0.1*M* sodium phosphate, 0.02% Nonidet P40, 0.01% deoxycholic acid, and 2 m*M* $MgCl_2$ [pH 7.4]). To detect β-galactosidase activity, tibial limbs and femurs were subsequently stained with X-Gal staining buffer (1 mg/ml X-Gal, 5 m*M* potassium ferricyanide, and 5 m*M* potassium ferrocyanide buffered with the washing buffer described above) for 36 hours. The femurs were additionally decalcified for 2 weeks with 10% EDTA (pH 7.4) at 4°C. After dehydration with an increasing concentration of ethanol and embedding in paraffin, they were sectioned into 4-μm slices. For immunohistochemistry, after treatment with 25 μg/ml hyaluronidase for 1 hour, sections were incubated overnight with rabbit polyclonal antibodies to rat type X collagen or with nonimmune serum (1:500 dilution; LSL, Tokyo, Japan). Localizations were detected with a horseradish peroxidase–conjugated secondary antibody (Promega, Madison, WI).

Construction of expression vectors. Full-length human RUNX-2 (accession no. NM_004348) complementary DNA (cDNA) and CBFβ (accession no. NM_022845) cDNA were amplified by polymerase chain reaction (PCR) and cloned into pCMV-HA (Clontech, Palo Alto, CA). RUNX-2 (accession no. NM_009820) cDNA and cDNA for a dominant-negative mutant of RUNX-2 (dnRUNX-2) were cloned into pMx vectors (27). A vector expressing dnRUNX-2 was generated by the form which contains the runt domain with N-terminal domain of RUNX-2 and lacks the C-terminal region, as previously described (19). Production of retrovirus vectors was performed as previously described (28,29). Plat-E cells (2×10^6) were plated in 60-mm dishes and transfected with 2 μg of pMx vector using FuGene 6 (Roche, Mannheim, Germany). After 24 hours, the medium was replaced with fresh medium, which was collected and used as the retrovirus supernatant 48 hours after transfection. The blasticidin resistance gene was inserted into the pMx vector of RUNX-2 and that of dnRUNX-2 for selection of stable cells.

Cell cultures. HeLa cells, HuH7 cells, COS-7 cells (RIKEN Cell Bank, Tsukuba, Japan), and OUMS27 cells (Health Science Research Resources Bank, Tokyo, Japan) were cultured in high-glucose Dulbecco's modified Eagle's medium (DMEM) with 10% fetal bovine serum (FBS). ATDC-5 cells (RIKEN Cell Bank) were grown and maintained in DMEM–Ham's F-12 (1:1) with 5% FBS. To induce hypertrophic differentiation, ATDC-5 cells were cultured in the presence of insulin–transferrin–sodium selenite supplement (Sigma, St. Louis, MO) for 3 weeks, and then with α-minimum essential medium/5% FBS with 4 m*M* inorganic phosphate for 2 days, as previously described (30). For generation of the stable cell lines, 3×10^5 ATDC-5 cells were plated and cultured in 60-mm dishes for 1 day, and the retrovirus supernatant was added to the cells with Polybrene (8 μg/ml final concentration). After 2 days, the cells were passaged into 100-mm dishes and cultured with medium containing 10 μg/ml blasticidin until confluency. For alizarin red staining, cultured cells were fixed in 10% buffered formalin and stained for 10 minutes with 2% alizarin red S (pH 4.0) (Sigma). For von Kossa's staining, cells were fixed with 100% ethanol for 15 minutes and stained with 5% silver nitrate solution under ultraviolet light for 5 minutes.

Reverse transcriptase–PCR (RT-PCR) and real-time RT-PCR analyses. Total RNA from cells was isolated with an RNeasy Mini kit, according to the recommendations of the manufacturer (Qiagen, Hilden, Germany), and 1 aliquot (1 μg) was reverse-transcribed with a QuantiTect Reverse Transcription kit (Qiagen) to make single-stranded cDNA. For RT-PCR, cDNA was amplified for 30 cycles in a PCR thermal cycler using Takara Ex *Taq* (Takara Bio, Shiga, Japan) and the following primer pairs: for the N-terminal region of RUNX-2, 5′-GCAAGATGAGCGACGTGAG-3′ and 5′-GTCCGCGATGATCTCCAC-3′; for the C-terminal region of RUNX-2, 5′-CCCAGCCACCTTTACCTACA-3′ and 5′-TATGGAGTGCTGCTGGTCTG-3′; and for β-actin, 5′-AGATGTGGATCAGCAAGCAG-3′and5′-GCGCAAGTTAGGTTTTGTCA-3′.

Real-time RT-PCR was performed with an ABI Prism 7000 Sequence Detection System (Applied Biosystems, Foster City, CA) using QuantiTect SYBR Green PCR Master Mix, according to the recommendations of the manufacturer (Qiagen). All reactions were run in triplicate. After data collection, the messenger RNA (mRNA) copy number of a specific gene in total RNA was calculated using a standard curve generated with serially diluted plasmids containing PCR amplicon sequences and normalized to rodent total RNA (Applied Biosystems) with mouse β-actin as an internal control. Standard plasmids were synthesized with a TOPO TA cloning kit, according to the recommendations of the manufacturer (Invitrogen, Carlsbad, CA). PCR amplification was performed using the following primer pairs: for type X collagen, 5′-CATAAAGGGCCCACTTGCTA-3′ and 5′-TGGCTGATATTCCTGGTGGT-3′; and for β-actin, 5′-AGATGTGGATCAGCAAGCAG-3′ and 5′-GCGCAAGTTAGGTTTTGTCA-3′.

Sequence search of COL10A1 promoters. A sequence search for the RUNX-2 binding motif was performed using Vector NTI (Invitrogen). To search sequences that were conserved between the human and mouse COL10A1 proximal promoters, we performed a BLASTN search (31) against the mouse genomic plus transcript database using a 4.5-kb fragment of the human COL10A1 5′-end flanking region.

Luciferase assay. The human COL10A1 promoter region from −4,459 bp to +39 bp relative to the transcription start site was obtained by PCR using human genomic DNA as a template and was cloned into the pGL3-Basic vector (Promega). Deletion and mutation constructs were created by PCR. Tandem repeat constructs were created by ligating double-stranded oligonucleotides into the pGL3-Basic vector. Transfection of HeLa, HuH7, OUMS27, and ATDC-5 cells was performed in triplicate in 48-well plates using FuGene 6 with plasmid DNA (100 ng of pGL3 reporter vector, 50 ng of effector vector, and 4 ng of pRL-TK vector [Promega]) for internal control per well. Cells were harvested 48 hours after transfection. Luciferase assay was performed with a dual luciferase reporter assay system (Promega) using a GloMax 96 microplate luminometer (Promega). Results were shown as the ratio of firefly activity to *Renilla* activity.

Electrophoretic mobility shift assay (EMSA). Nuclear extracts were obtained from COS-7 cells overexpressing empty vector, RUNX-2, or the combination of RUNX-2 and CBFβ 48 hours after transfection using NE-PER, according to the recommendations of the manufacturer (Pierce, Rockford, IL). Each expression vector was transfected using FuGene 6. EMSA was carried out using a DIG Gel Shift kit, according to the recommendations of the manufacturer (Roche). Binding reactions were incubated for 30 minutes at room temperature. For competition analyses, a 100-fold excess of unlabeled competitor probe was included in the binding reaction. For the supershift experiments, 1 μl of anti–RUNX-2 antibody (M-70 X; Santa Cruz Biotechnology, Santa Cruz, CA) was added after 30 minutes of binding reaction, and the reaction was incubated for an additional 30 minutes at room temperature. Samples were loaded onto Novex 6% Tris–borate–EDTA gels (Invitrogen) and electrophoresed at 100V for 60 minutes.

Chromatin immunoprecipitation (ChIP) assay. A ChIP assay was performed with a OneDay ChIP kit, according to the recommendations of the manufacturer (Diagenode, Liège, Belgium). HuH7 cells were transfected with empty vector and the combination of RUNX-2 and CBFβ using FuGene 6. In vivo crosslinking was performed 48 hours after transfection. To shear genomic DNA, the lysates were then sonicated on ice 10 times for 30 seconds each. For immunoprecipitation, anti–RUNX-2 antibody (M-70 X) and normal rabbit IgG (negative control; Promega) were used.

RESULTS

Localization of RUNX-2 and type X collagen during endochondral ossification. We initially examined the in vivo expression patterns of RUNX-2 and type X collagen during endochondral ossification in skeletal growth and repair using specimens of limb cartilage from neonatal mice and bone fracture callus from adult mice (Figure 1). Due to the lack of appropriate and sensitive antibodies or riboprobes to examine RUNX-2 localization in wild-type mouse cartilage tissue, we used X-Gal staining in heterozygous *Runx2*-deficient mice with the *lacZ* gene insertion at the *Runx2*-deletion site ($Runx2^{+/lacZ}$) (32). RUNX-2 was widely expressed in cartilage and bone areas, but was expressed most strongly in hypertrophic chondrocytes in both specimens. Strong RUNX-2 expression was well colocalized with the area of positive immunostaining with type X collagen, consistent with the results we previously reported for OA cartilage (22) and confirming the molecular interaction between RUNX-2 and type X collagen during endochondral ossification.

Functional role of RUNX-2 in type X collagen expression and terminal differentiation of cultured chondrocytes. To investigate the function of RUNX-2 during endochondral ossification, we examined the effects of gain and loss of function of RUNX-2 on mouse chondrogenic ATDC-5 cells that were cultured in differentiation medium (30). For the gain-of-function analysis, we established stable lines of ATDC-5 cells overexpressing RUNX-2 or the empty vector through retroviral

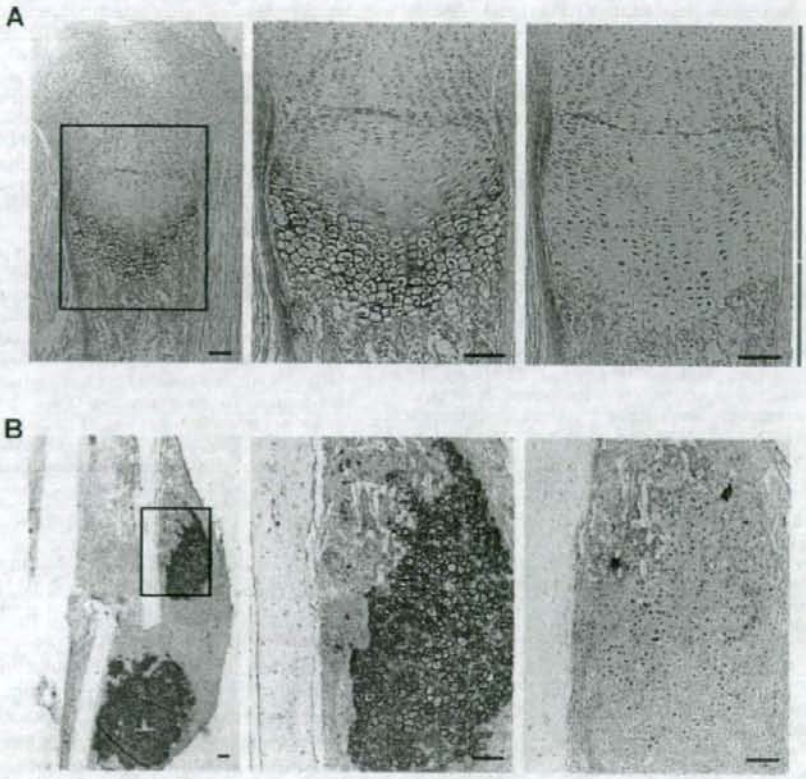

Figure 1. Expression of runt-related transcription factor 2 (RUNX-2) and type X collagen in **A**, the proximal tibial limb cartilage of 1-day-old neonatal mice and **B**, the bone fracture callus of 8-week-old adult mice 9 days after osteotomy at the femur midshaft. Specimens from heterozygous *Runx*2-deficient mice with the RUNX-2 promoter and *lacZ* gene knockin at the *Runx2* deletion site ($Runx2^{+/lacZ}$ mice) were stained with X-Gal and antibody to type X collagen (left and middle) or with X-Gal and nonimmune control serum (right). RUNX-2 localization is shown as blue X-Gal staining to detect β-galactosidase activity. Type X collagen localization is shown as brown immunostaining with an antibody to type X collagen. The middle and right panels show higher-magnification views of the boxed areas in the left panels. The blue, red, and green bars in **A** indicate layers of proliferative zone, hypertrophic zone, and bone area, respectively. Bars = 100 μm.

transfection and found that the type X collagen mRNA level as well as the terminal differentiation determined by alizarin red and von Kossa's stainings were potently stimulated by RUNX-2 overexpression (Figure 2A).

Next, to determine the effects of loss of function of RUNX-2, we established stable lines of ATDC-5 cells overexpressing a dominant-negative mutant of RUNX-2 that lacks the C-terminal region (19), which were cultured in differentiation medium (Figure 2B). The type X collagen mRNA level and the intensity of the stainings were decreased by the overexpression, indicating that RUNX-2 is a crucial factor for type X collagen expression and terminal differentiation of chondrocytes.

Transactivation of the human COL10A1 promoter by RUNX-2 and identification of the responsive element. To examine the mechanism underlying the induction of type X collagen expression by RUNX-2 in humans, we initially compared sequences of the 4.5-kb fragment of the 5′-end flanking region of the human COL10A1 gene with the corresponding mouse genes

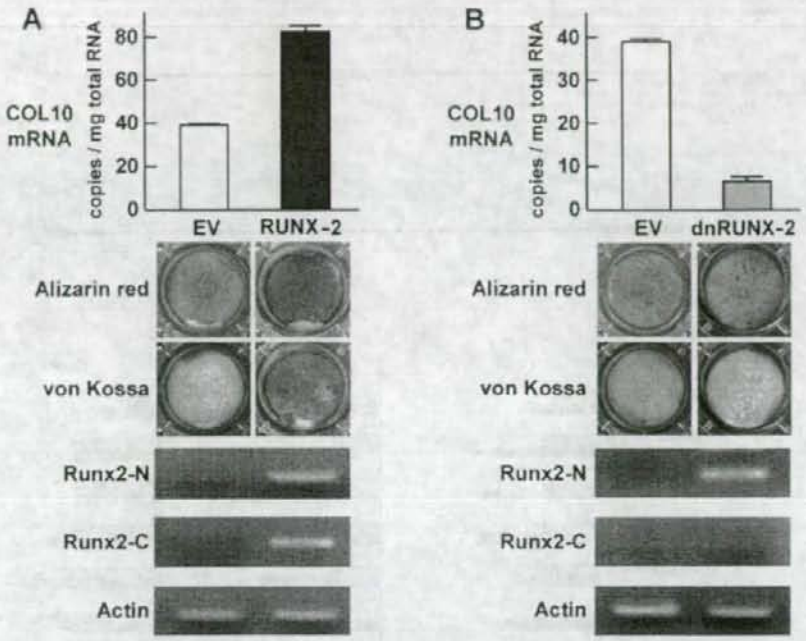

Figure 2. Effect of gain and loss of function of runt-related transcription factor 2 (RUNX-2) on type X collagen (COL10) expression and terminal differentiation in cultured mouse chondrogenic ATDC-5 cells. **A,** Type X collagen mRNA level, determined by real-time reverse transcriptase–polymerase chain reaction (RT-PCR), and alizarin red and von Kossa's staining in stable lines of ATDC-5 cells retrovirally transfected with empty vector (EV; control) or with RUNX-2 after culture for 3 weeks with insulin–transferrin–sodium selenite and for 2 days with inorganic phosphate. **B,** Type X collagen mRNA level, determined by RT-PCR, and alizarin red and von Kossa's staining in stable lines of ATDC-5 cells retrovirally transfected with empty vector or with dominant-negative RUNX-2 (dnRUNX-2), which contains the N-terminal region (Runx2-N), but not the C-terminal region (Runx2-C) of RUNX-2, under the same culture conditions as in A. Gene expression of RUNX-2 and dnRUNX-2 was confirmed by RT-PCR analysis using 2 primer sets for the N-terminal region and the C-terminal region of RUNX-2. Bars show the mean and SD of 3 wells per group.

(Figure 3A). The sequences were substantially different, except for 2 regions that were ≥70% conserved between the species.

We then analyzed the promoter activity of the human COL10A1 gene using 3 human cell lines, epithelial HeLa cells, hepatic HuH7 cells, and chondrogenic OUMS27 cells, that were transfected with a luciferase reporter gene construct containing the 4.5-kb fragment of the 5′-end flanking region of the COL10A1 gene and the series of deletion fragments (Figure 3B). The transcription activity determined by the luciferase reporter assay was enhanced by cotransfection with RUNX-2 and more potently by cotransfection with both RUNX-2 and the coactivator CBFβ as compared with the control empty vector, confirming activation of the COL10A1 promoter by RUNX-2 and enhancement by the CBFβ cotransfection in all cell lines. Deletion analysis by a series of 5′-deletion constructs identified the responsive region to RUNX-2 as being between −81 bp and −76 bp, containing a putative RUNX-2 binding sequence (TGAGGG), which is similar to that identified in the promoter region of human interleukin-3 (TGTGGG) (33). This was within the highly conserved region in the comparative mapping described above (Figure 3A).

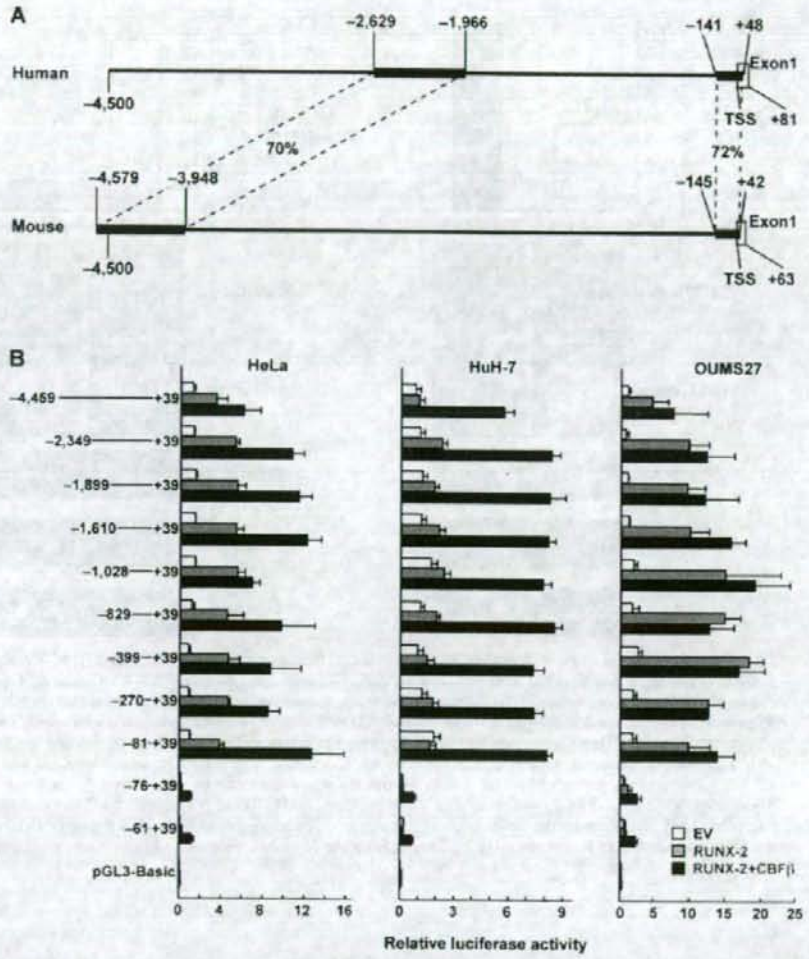

Figure 3. A, Comparison of sequences of COL10A1 proximal promoter regions in human and mouse genes. The 4.5-kb fragment of the human 5′-end flanking region was compared with the mouse genomic plus transcript database. **B,** Luciferase assays for human COL10A1 promoter activity induced by transfection with RUNX-2 and identification of the responsive region by deletion analysis in human cells. Three human cell lines, epithelial HeLa cells, hepatic HuH7 cells, and chondrogenic OUMS27 cells, transfected with luciferase reporter constructs containing a 5′-end flanking region of the human COL10A1 gene (from −4,459 bp to +39 bp relative to the transcription start site) and the series of deletion fragments were cotransfected with empty vector (control), RUNX-2 alone, or RUNX-2 and core-binding factor β (CBFβ). Bars show the mean and SD relative luciferase activity (ratio of firefly activity to *Renilla* activity) of 3 wells per group. TSS = transcription start site (see Figure 2 for other definitions).

We therefore prepared the 30-bp element (from −89 to −60 bp) containing the identified region for further analyses, and called it the hypertrophy box (HY box) (Figure 4). To determine the core responsive element in the HY box, we performed site-directed mutagenesis analysis of the luciferase assay by creating 3

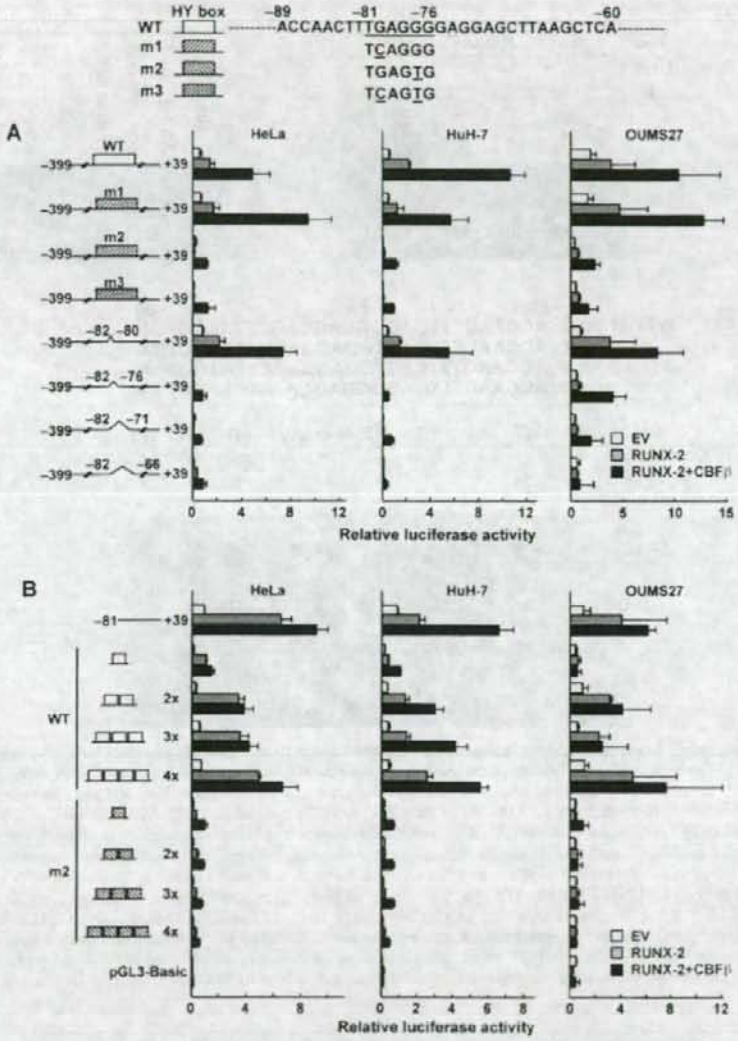

Figure 4. Luciferase assays for determination of the core responsive element in the hypertrophy box (HY box; −89 bp to −60 bp) containing the identified responsive region (from −81 bp to −76 bp, underlined) in the human COL10A1 promoter by site-directed mutagenesis (underlined) and deletion, and dose-response analysis of the tandem repeats using 3 human cell lines cotransfected with empty vector (control), RUNX-2 alone, or RUNX-2 and the coactivator core-binding factor β (CBFβ). **A,** Single-base mutations (m1 and m2), a double-base mutation (m3), and 1–15-bp deletions starting at the −81 bp site were created in the HY box of the 5'-end flanking region between −339 bp and +39 bp, and luciferase activity was compared with that in the wild-type (WT) HY box. **B,** Dose-response analysis of the tandem repeats of the WT and the mutated (m2) HY box was performed. Bars show the mean and SD relative luciferase activity of 3 wells per group. See Figure 2 for other definitions.